

# Effects of FeO and CaO/Al<sub>2</sub>O<sub>3</sub> Ratio in Slag on the Cleanliness of Al-Killed Steel



YUNQING JI, CHUNYANG LIU, YAN LU, HUIXIANG YU, FUXIANG HUANG,  
and XINHUA WANG

The slag composition plays a critical role in the formation of inclusions and the cleanliness of steel. In this study, the effects of FeO content and the C/A (CaO/Al<sub>2</sub>O<sub>3</sub>) ratio in the slag on the formation of inclusions were investigated based on a 10-minute slag–steel reaction in a MgO crucible. The FeO content in the top slag was shown to have a significant effect on the formation of MgO·Al<sub>2</sub>O<sub>3</sub> spinel inclusions, and critical content exists; when the initial FeO content in the slag was less than 2 pct, MgO·Al<sub>2</sub>O<sub>3</sub> spinel inclusions formed, and the T.O (total oxygen) was 20 ppm; when the initial FeO content in the slag was more than 4 pct, only Al<sub>2</sub>O<sub>3</sub> inclusions were observed and the T.O was 50 ppm. It was clarified that the main source of Mg for the MgO·Al<sub>2</sub>O<sub>3</sub> spinel inclusion formation was the top slag rather than the MgO crucible. In addition, the cleanliness of the steel increased as the initial FeO content in the top slag decreased. As regards the effects of the C/A ratio, the MgO amount in the observed inclusions gradually increased, whereas the T.O content decreased gradually with the increasing C/A ratio. Slag with a composition close to the CaO-saturated region had the best effect on the inclusion absorption.

<https://doi.org/10.1007/s11663-018-1397-2>

© The Minerals, Metals & Materials Society and ASM International 2018

## I. INTRODUCTION

WITH the recent increase in demand for high-quality steel, the requirements for steel with higher cleanliness have become more stringent. Inclusions, which are normally determined as impurities, can cause many defects and degrade the properties of the steel product. Inclusions are directly determined based on the steel composition, whereas the steel composition is further affected by the refining of the slag and the refractory material. Therefore, the properties of the slag play very important roles in the formation of inclusions and in the improvement of the cleanliness in the steel.

For the production of interstitial-free (IF) steel, the steel melt is generally created through the BOF-RH-CC process. During the tapping of the steel after BOF refining, the BOF slag with high amounts of FeO and

MnO is easily poured into the ladle along with the steel. According to measures taken with regard to the slag carry-over, the subsequent RH process is divided into two processes. In the first process, the slag deoxidizer and the slag former are added into the steel during the tapping process, and the oxygen potential of the top slag is decreased. During the second process, the residue of the BOF slag continues to react with the steel, and no slag deoxidant is added. A number of researchers<sup>[1–6]</sup> have investigated the cleanliness and inclusions formed in steel through these two processes. At Sumitomo,<sup>[1,2]</sup> researchers studied the effects of slag oxidation on the Al loss during steel deoxidation at 10 kg and 250 t scales. Al loss increases from 1 to 3 ppm/min when the FeO content in the slag increases from 5 pct (all compositions in this paper are given in mass percentages unless specifically stated otherwise) to 10 pct. A large number of slivers present in the final products have been traced to the reoxidation originating from FeO in the ladle slag, and Lee *et al.*<sup>[3]</sup> and Kitamura *et al.*<sup>[4]</sup> have shown that the number of defects on cold-rolled sheets diminishes with a diminishing FeO + MnO ladle slag content at the end of the secondary metallurgy treatments. Qin *et al.*<sup>[5]</sup> found that the cleanliness of steel refined through slag with a lower oxygen potential (FeO 7 to 9 pct) is much better than that refined using slag with a higher oxygen potential (FeO 21 pct). They concluded that the FeO amount should be reduced to improve the cleanliness of the steel. The same

YUNQING JI, HUIXIANG YU, and XINHUA WANG are with the School of Metallurgical and Ecological Engineering, University of Science and Technology Beijing, 30 Xueyuan Road, Haidian District, Beijing, 100083, P.R. China. Contact e-mail: yuhuixiang@ustb.edu.cn CHUNYANG LIU and YAN LU are with the Department of Metallurgy, Graduate School of Engineering, Tohoku University, 2-1-1 Katahira, Aoba-ku, Sendai, 980-8577, Japan. FUXIANG HUANG is with the Steelmaking Plant of Beijing Shougang Co., Ltd., Qian'an, 100041, Hebei, P.R. China.

Manuscript submitted May 1, 2018.

Article published online September 7, 2018.

phenomenon was observed by other researchers.<sup>[6]</sup> However, the interaction mechanism between Al-killed steel and FeO in slag remains unclear. In addition, the refining slag also contains MgO, which helps relieve the refraction erosion by the slag. The MgO in the slag can be reduced by Al in the steel, and the resultant Mg, which reacts with the existing Al<sub>2</sub>O<sub>3</sub> inclusions in the steel, forms spinel inclusions.<sup>[7-9]</sup> A number of researchers<sup>[8-13]</sup> have found that the MgO content in the inclusions increases as the FeO content in the slag decreases. When the FeO + MnO amount is more than 2 to 3 pct, the MgO content in the inclusions is nearly less than 5 pct. However, based on a thermodynamic calculation, a reduction of MgO by Al in the steel cannot occur even if the FeO amount in the slag is as low as 1 to 2 pct.

Apart from reoxidation, the inclusion-absorption capability of refined slag can also affect the cleanliness of the steel. A number of researchers<sup>[14-17]</sup> have investigated the inclusion-absorption capacity of slag. The removal of nonmetallic particles occurs in three stages: flotation, separation, and dissolution. To obtain clean steel, the slag must satisfy two basic requirements: it must exhibit substantial wettability with inclusions, and provide high inclusion dissolution rates. The contact angle determines the wettability between the inclusion and slag. Choi and Lee<sup>[14]</sup> measured the contact angle between the CaO-Al<sub>2</sub>O<sub>3</sub>-SiO<sub>2</sub> slag system and Al<sub>2</sub>O<sub>3</sub> inclusions using a sessile drop method. They found that the contact angle decreased with the increasing C/A ratio, which indicates a better wettability. Choi *et al.*<sup>[15]</sup> investigated the dissolution rate of Al<sub>2</sub>O<sub>3</sub> into molten CaO-SiO<sub>2</sub>-Al<sub>2</sub>O<sub>3</sub> slag, and found that the dissolution of Al<sub>2</sub>O<sub>3</sub> into a CaO-SiO<sub>2</sub>-Al<sub>2</sub>O<sub>3</sub> slag system was controlled by the mass transfer during the slag phase. Valdez<sup>[16]</sup> investigated the capability of slag to absorb solid oxide inclusions. They found that the inclusion dissolution time has a reciprocal relation with the  $\Delta C/\eta$  (where  $\Delta C$  is the super saturation, and  $\eta$  is the slag viscosity). Based on the value of  $\Delta C/\eta$ , the liquid area of CaO-SiO<sub>2</sub>-Al<sub>2</sub>O<sub>3</sub> at 1873 K was divided into four distinct regions. The slag closest to the CaO saturation region exhibited the best performance of Al<sub>2</sub>O<sub>3</sub> inclusion absorption. Monaghan and Chen<sup>[18]</sup> investigated the effects of changing the slag composition on the spinel inclusion dissolution. They found that the mechanism of spinel inclusion dissolution was at least in part controlled through the mass transfer during the slag phase. However, most of the studies above focused on the fundamental elements of inclusion absorption into the slag such as the kinetics and thermodynamics. There have been a limited number of reports on the effects of the slag composition on steel cleanliness, which has a more direct influence on the quality of a steel product.

In this study, Al-killed steel was reacted with CaO-Al<sub>2</sub>O<sub>3</sub>-SiO<sub>2</sub>-MgO-FeO slag in a MgO crucible, and the effects of the FeO content and C/A ratio on the inclusion formation behavior and steel cleanliness were clarified.

## II. EXPERIMENTAL METHOD

### A. Raw Materials

The steel employed in this study was IF steel. Because the Al loss after the slag-steel reaction was significant, the Al content in the IF steel was adjusted to 0.08 pct by remelting the IF steel in an Al<sub>2</sub>O<sub>3</sub> crucible. The inclusion type in the steel after the Al adjustment was only Al<sub>2</sub>O<sub>3</sub>, and the MgO amount in the observed inclusions was zero.

To prepare the slag, FeO was prepared by melting Fe<sub>2</sub>O<sub>3</sub> and Fe powder in a Fe crucible at 1673 K for 1 hour, with a ratio of mixed Fe<sub>2</sub>O<sub>3</sub> to Fe of 1:1. The FeO was subsequently mixed with reagent grade MgO, CaO, Al<sub>2</sub>O<sub>3</sub>, and SiO<sub>2</sub>.

### B. Experiment Procedure

The experiment setup used is shown in Figure 1. The experiment was conducted using an electrical resistance furnace with Si-Mo heating. Prior to heating, 180 g of the prepared metal, along with 7.2 g of the slag mixture, was loaded into a dense MgO crucible (ID, 38 mm; OD, 44 mm; *H*, 136 mm). Then, the chamber of the furnace was purged with Ar gas for a given period of time. Subsequently, the metal was heated to 1873 K, which was considered the starting point of the experiment. Following the slag-steel reaction for 10 minutes, the molten steel along with the slag and crucible was rapidly quenched with water.

To clarify the influence of the FeO content on the inclusion formation, experiments were conducted using 2, 4, and 11 pct of FeO in the slag. In addition, to clarify the influence of the C/A ratio, experiments were conducted with C/A ratios of 0.5, 1.0, 1.5, 2.0, and 2.5. The experimental conditions applied are listed in Table I.

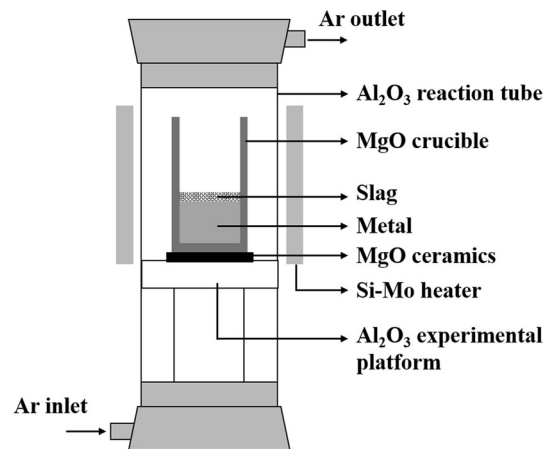


Fig. 1—Experiment setup.

**Table I. Experimental Conditions**

| Experimental No. | Initial Al Content in Steel (Mass Pct) | Slag Composition (Mass Pct) |                  |                                |     |      |                                    |
|------------------|--|-----------------------------|------------------|--------------------------------|-----|------|------------------------------------|
|                  |  | CaO                         | SiO <sub>2</sub> | Al <sub>2</sub> O <sub>3</sub> | MgO | FeO  | CaO/Al <sub>2</sub> O <sub>3</sub> |
| 1                | 0.078                                  | 48.5                        | 8.1              | 32.4                           | 9.0 | 2.0  | 1.5                                |
| 2                | 0.076                                  | 47.5                        | 7.9              | 31.6                           | 9.0 | 4.0  | 1.5                                |
| 3                | 0.088                                  | 43.6                        | 7.3              | 29.1                           | 9.0 | 11.0 | 1.5                                |
| 4                | 0.083                                  | 28.1                        | 4.7              | 56.2                           | 9.0 | 2.0  | 0.5                                |
| 5                | 0.078                                  | 41.1                        | 6.8              | 41.1                           | 9.0 | 2.0  | 1.0                                |
| 6                | 0.078                                  | 53.4                        | 8.9              | 26.7                           | 9.0 | 2.0  | 2.0                                |
| 7                | 0.083                                  | 56.8                        | 9.5              | 22.7                           | 9.0 | 2.0  | 2.5                                |

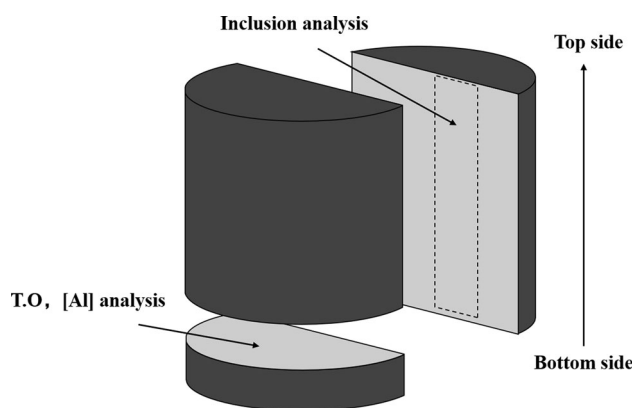


Fig. 2—Schematic of a cut sample.

### C. Analysis

Following quenching, the steel sample was cut for both a chemical composition analysis and an observation of the inclusions. A schematic of a cut sample is shown in Figure 2. For the chemical analysis, the Al content was analyzed using inductively coupled plasma atomic emission spectroscopy (ICP-AES). Because the Mg content in the steel was too low for an accurate analysis, no information of the Mg in the steel is provided in the present paper. The T.O of the steel sample was measured using an infrared X-ray absorption method, and the FeO content in the slag was measured using an oxidation–reduction titration method. To observe the inclusions, a scanning electron microscope (SEM) equipped with an automatic inclusion analysis system was used (P-SEM, ASPEx Co.). For the P-SEM observations, the accelerating voltage used for the EDS analysis of the inclusions was 20 kV. During the P-SEM analysis, Mg, Al, Fe, Ti, Ca, Si, and O were selected as the target elements because they exist in the molten steel sample. In this study, only Mg, Al, Ti, and O were detected in the observed inclusions. Thus, the inclusions were assumed to consist of Al<sub>2</sub>O<sub>3</sub>, Ti<sub>2</sub>O<sub>3</sub>, and MgO, and the analyzed values of Al, Ti, and Mg were converted into oxide values based on the stoichiometric relationship. The O was detected to confirm whether the observed material was oxide and not metal. During a pre-experiment, inclusions of larger than 2 and 5 μm were detected during the P-SEM observations. The average amounts of MgO, Al<sub>2</sub>O<sub>3</sub>, and TiO<sub>2</sub> in the observed inclusions for these two cases were

almost the same. Thus, in this study, only inclusions of larger than 5 μm were detected to save the time for the P-SEM observation.

## III. EXPERIMENT RESULTS

The distributions of inclusions observed during experiments 1 to 3 are shown in Figure 3. When the initial FeO amount in the slag was 2 pct, both Al<sub>2</sub>O<sub>3</sub> and spinel inclusions were mostly observed, with the exception of some Al<sub>2</sub>O<sub>3</sub>-Ti<sub>2</sub>O<sub>3</sub> inclusions. The formation of these Al<sub>2</sub>O<sub>3</sub>-Ti<sub>2</sub>O<sub>3</sub> inclusions is beyond the scope of the present study. The initial inclusions in the steel were pure Al<sub>2</sub>O<sub>3</sub>, and after the reaction, MgO·Al<sub>2</sub>O<sub>3</sub> spinel inclusions formed. For the Mg source of the spinel inclusion formation, both MgO in the slag and MgO in the crucible were taken into consideration. A number of researchers<sup>[8,19]</sup> have investigated the Mg dissolution rate from a slag and crucible. If the MgO in the crucible is reduced by the Al in the steel and the Mg supplied, a MgO·Al<sub>2</sub>O<sub>3</sub> spinel layer will form on the crucible surface. The elemental mapping of the reacted crucible–steel is shown in Figure 4. No Al was observed at the interface of the crucible and steel, which indicates that the Mg source for the spinel inclusion generation was the top slag. When the initial FeO in the slag content was more than 4 pct, only Al<sub>2</sub>O<sub>3</sub> inclusions were observed, and the distribution of the inclusions formed was uniform. The typical morphology of the inclusions observed during the slag–steel reaction for experiments 1 to 3 is shown in Figure 5. Al<sub>2</sub>O<sub>3</sub> inclusions with a dendrite shape, which are usually observed during the deoxidation process when significant oversaturation occurs, were also observed during this reoxidation process. The average MgO amount in the observed inclusions and the T.O content in steel after the reaction for experiments 1 to 3 are shown in Figures 6 and 7, respectively. When the MgO amount in the inclusions is greater than 29 pct, it is determined to be MgO-saturated spinel; and when the MgO amount in the inclusions is lower than 19 pct, it is determined to be Al<sub>2</sub>O<sub>3</sub>-saturated spinel. As the results indicate, it is evident that a critical amount of FeO of between 2 and 4 pct exists to promote the spinel inclusion formation. When the initial FeO content in the slag was less than 2 pct, MgO·Al<sub>2</sub>O<sub>3</sub> spinel inclusions formed, and the T.O was 20 ppm after a 10-minute reaction. When the initial FeO content in the slag was more than 4 pct, only Al<sub>2</sub>O<sub>3</sub> inclusions were observed, and the T.O was 50 ppm. The changes in Al

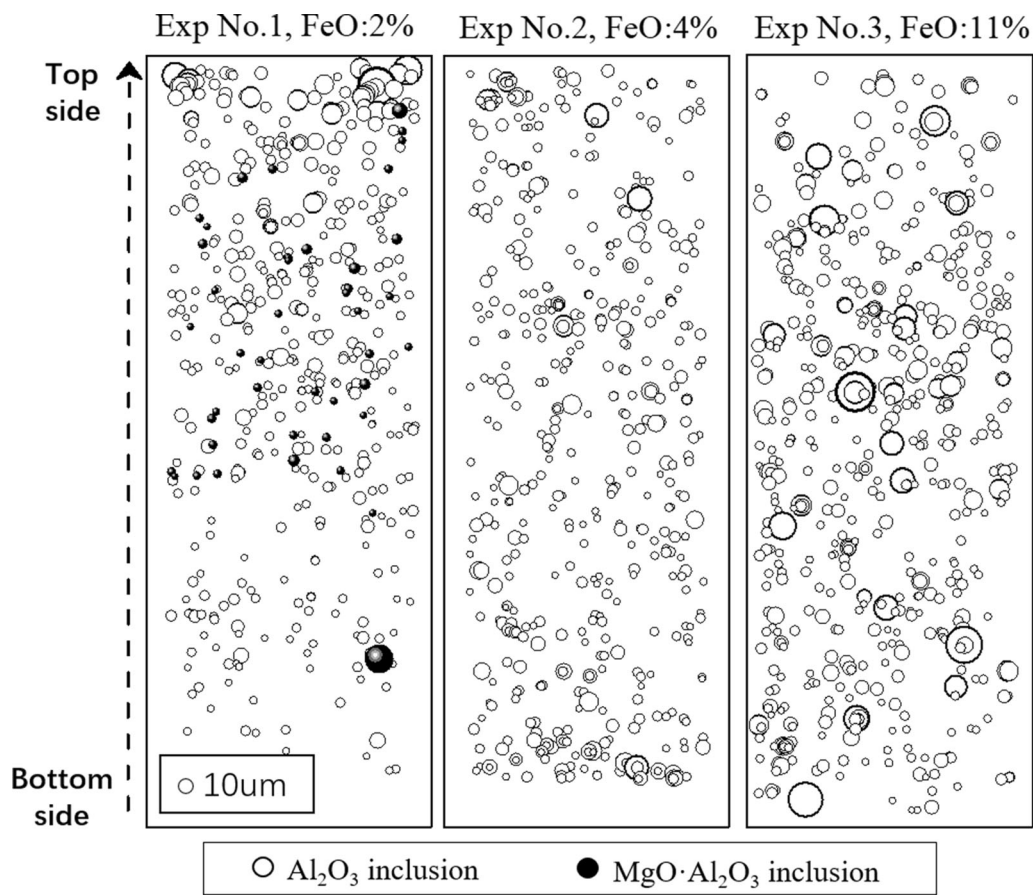


Fig. 3—Distributions of the observed inclusions for experiments 1–3.

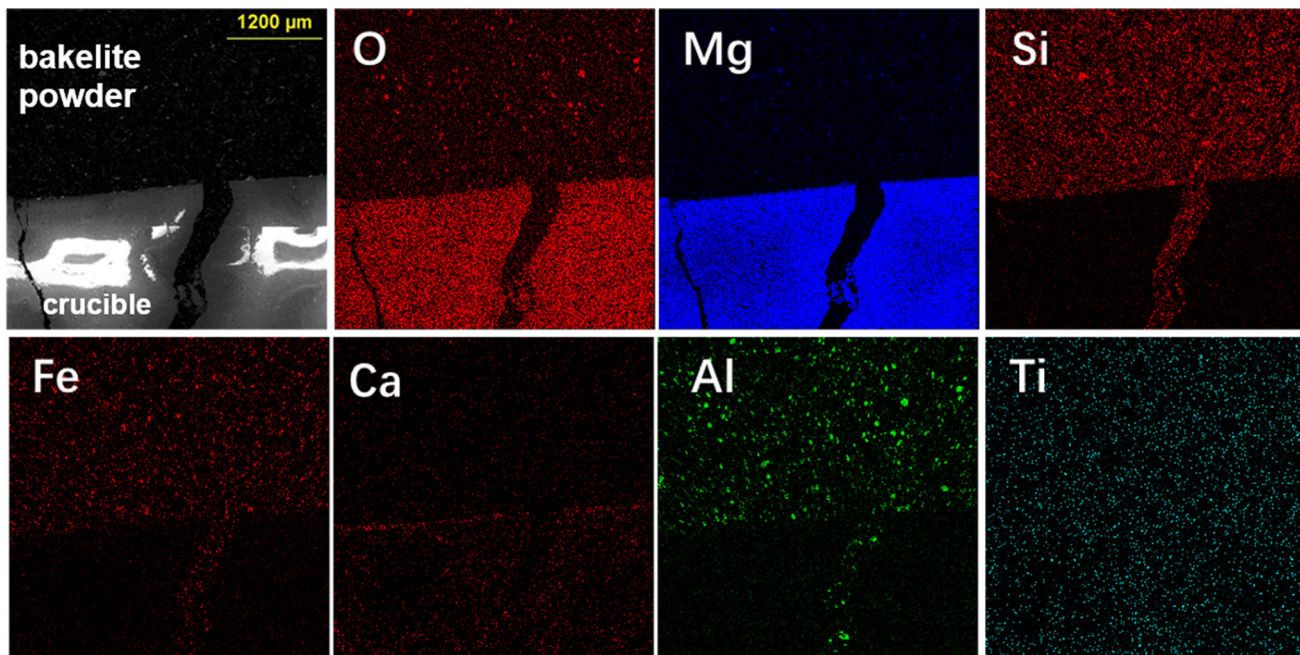


Fig. 4—Elemental mapping of the reacted crucible–steel.

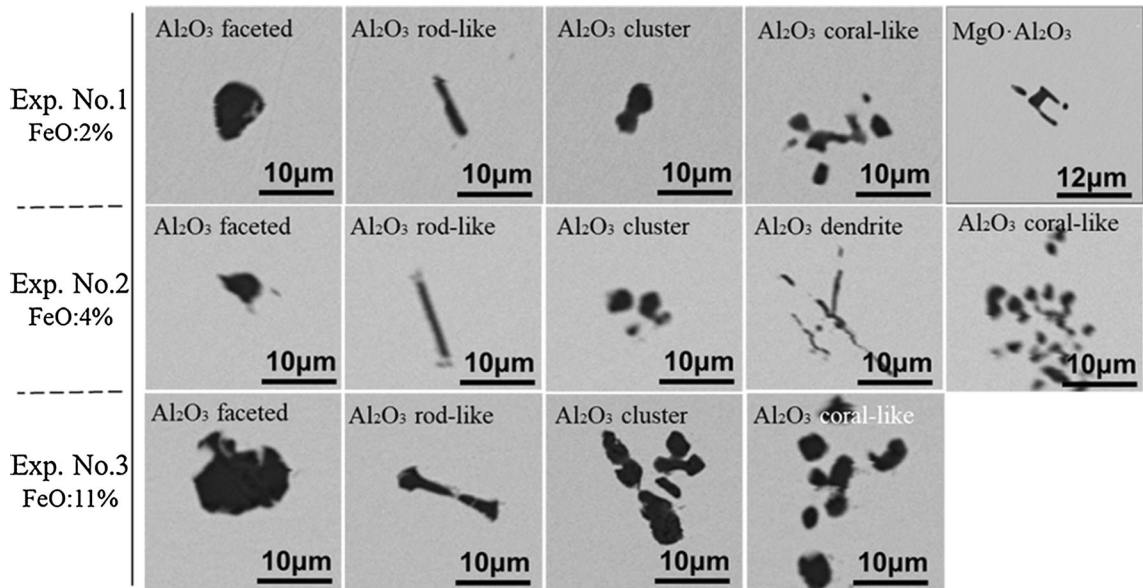


Fig. 5—Typical morphology of the inclusions observed for experiments 1–3.

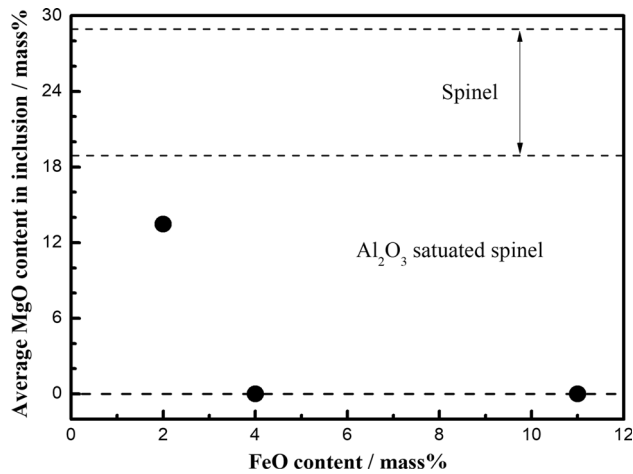


Fig. 6—Average MgO amount in inclusions observed for experiments 1–3.

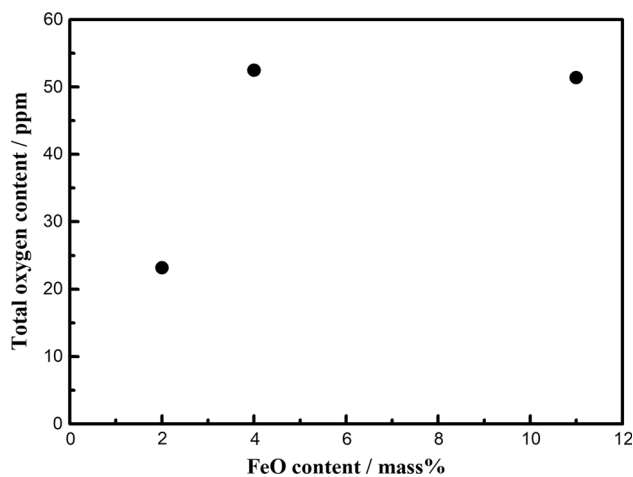


Fig. 7—Total oxygen content in the steel after the reaction.

content in steel and the FeO content in slag during the reaction are shown in Table II, and it is evident that the Al loss increases with the increasing initial FeO content in the slag. As the slag was difficult to collect for measurements after the reaction, the FeO content in the slag after the reaction was absent in some of the experiments.

The distributions of the observed inclusions for experiments 1 and 4 to 7 are shown in Figure 8. Both  $\text{Al}_2\text{O}_3$  and spinel inclusions were formed, and the distributions of the inclusions were nearly uniform during all experiments. In addition, the number of inclusions observed decreased significantly with the increasing C/A ratio. The typical morphology of the inclusions observed after the slag–steel reaction for experiments 1 and 4 to 7 is shown in Figure 9, which is nearly the same as that in the previous experiment conducted on the influence of FeO. The average MgO amount in the inclusions observed and the T.O content in steel after the reaction for experiments 1 and 4 to 7 are shown in Figures 10 and 11, respectively. From Figure 10, it is clear that the average MgO amount in the inclusions observed increased gradually, and the inclusions changed from  $\text{Al}_2\text{O}_3$ -saturated spinel into spinel inclusions with the C/A ratio. As shown in Figure 11, the T.O content decreased gradually with the increasing C/A ratio. Because the FeO amount in these experiments was the same (2 pct), the only reason for the decrease in T.O is that the inclusion-absorption capability of the slag increased with the C/A ratio.

#### IV. DISCUSSION

The top slag supplied Mg and O to the Al-killed steel through Reactions [1] and [2]. For the supply of Mg, the MgO in both the crucible and top slag could be the source. However, the absence of Al at the crucible–steel

Table II. Changes of Al Content and FeO Content During Reaction

| Experimental No. | Al Content Before Reaction (Mass Pct) | Al Content After Reaction (Mass Pct) | FeO Content Before Reaction (Mass Pct) | FeO Content After Reaction (Mass Pct) |
|------------------|---------------------------------------|--------------------------------------|--|---------------------------------------|
| 1                | 0.078                                 | 0.034                                | 2.0                                    | 0.64                                  |
| 2                | 0.076                                 | 0.038                                | 4.0                                    | —                                     |
| 3                | 0.088                                 | 0.005                                | 11.0                                   | —                                     |
| 4                | 0.083                                 | 0.054                                | 2.0                                    | —                                     |
| 5                | 0.078                                 | 0.04                                 | 2.0                                    | 0.6                                   |
| 6                | 0.078                                 | 0.032                                | 2.0                                    | 3.68                                  |
| 7                | 0.083                                 | 0.022                                | 2.0                                    | —                                     |

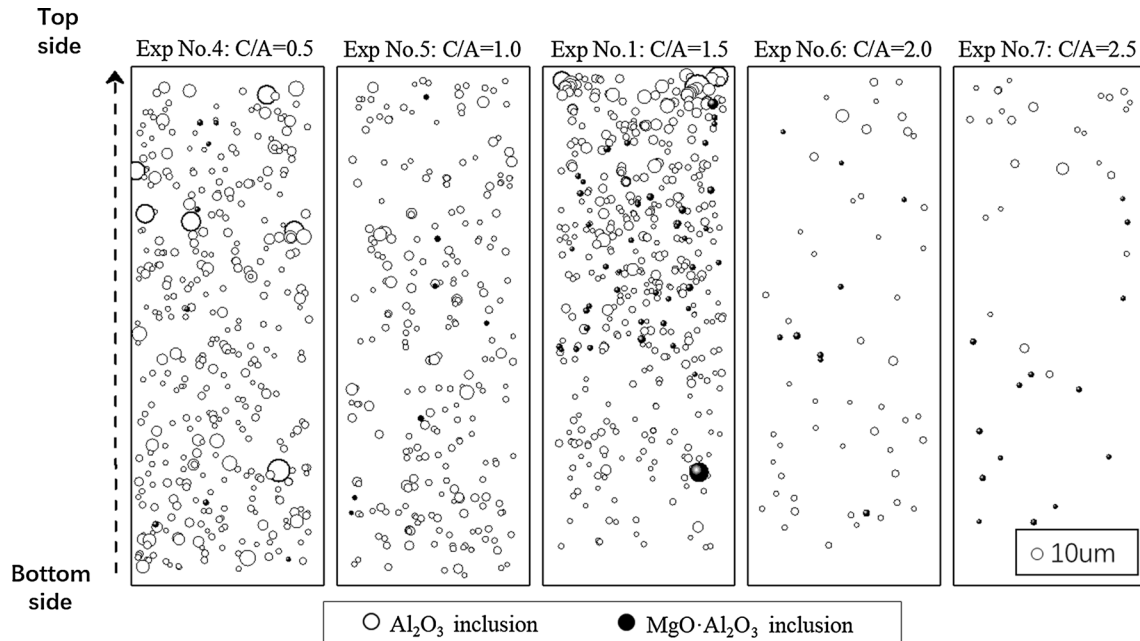
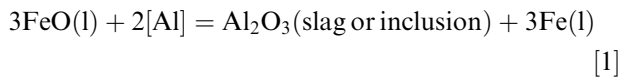
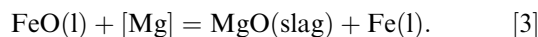


Fig. 8—Distribution of the inclusions observed for experiments 1 and 4–7.

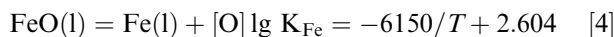
interface indicated that only the top slag was the main source of Mg for the spinel formation. Therefore, only MgO in the slag was considered in this study.



At the slag–steel interface, Reactions [1] and [2] could have occurred simultaneously, and there is another possibility that Reaction [1] has a priority to occur, which means the supplied Mg reduced FeO through Reaction [3].



The equilibrium constant of these reactions can be calculated through Reactions [4] to [6]. However, many results have been published for Reaction [6], as shown in Table III.<sup>[20–23]</sup>



The Mg content equilibrated with the FeO-containing top slag is shown in Figure 12. During the calculation, the steel composition is assumed to be Al 0.08 pct, O 10 ppm, and Ti 0.05 pct, and the cited activity interaction coefficient is shown in Table IV.<sup>[24]</sup> All of the component activities in top slag were calculated using FactSage.

As shown in Figure 12, the Mg content decreased with the FeO amount in the slag, and the calculated Mg content even varied with the different amounts of  $K_{\text{Mg}}$ . The calculated results were nearly less than 1 ppm despite the FeO amount in the slag being as low as 1 pct, which indicates that Reaction [1] has the priority of occurrence, and Reaction [2] does not occur when FeO has not decreased to an extremely low content. The

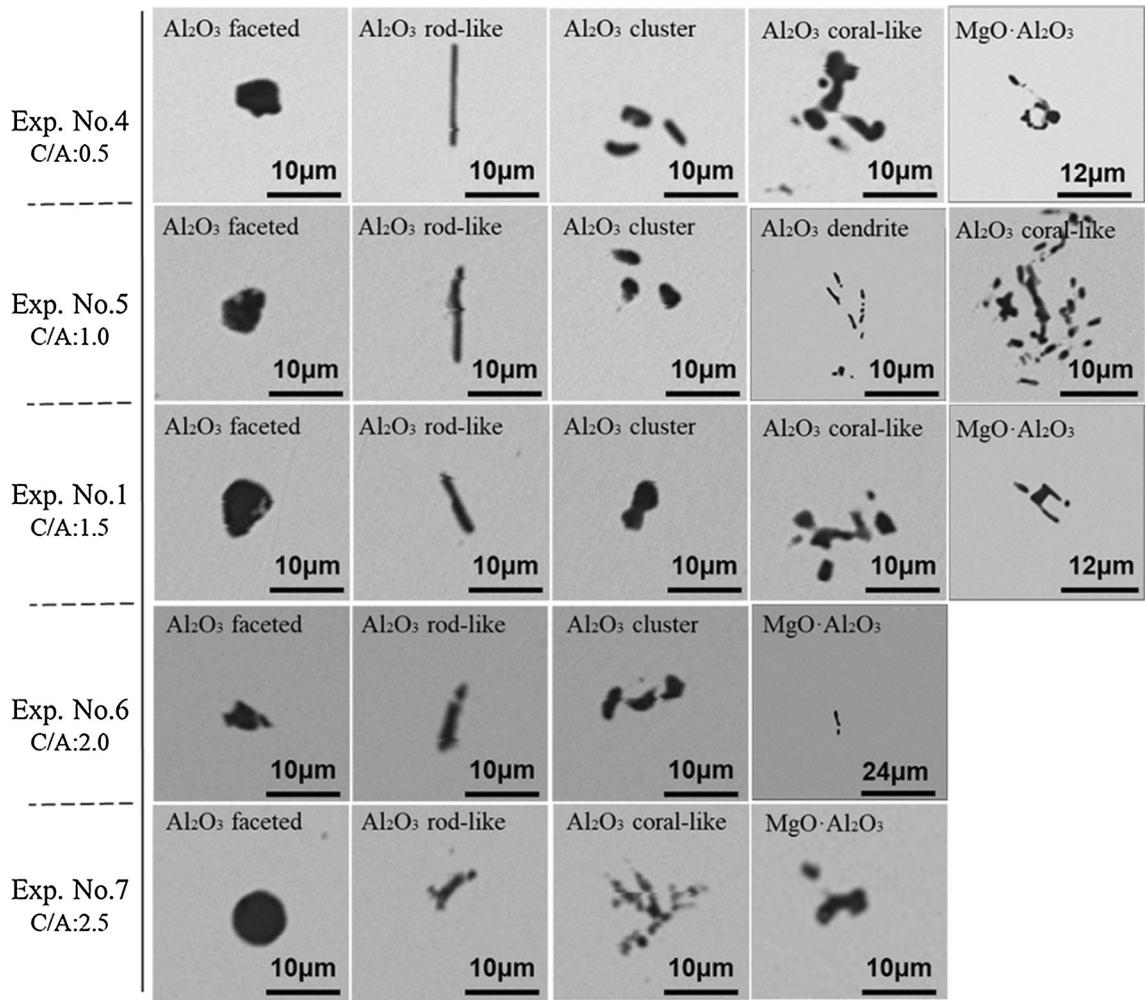


Fig. 9—Typical morphology of the inclusions observed for experiments 1 and 4–7.

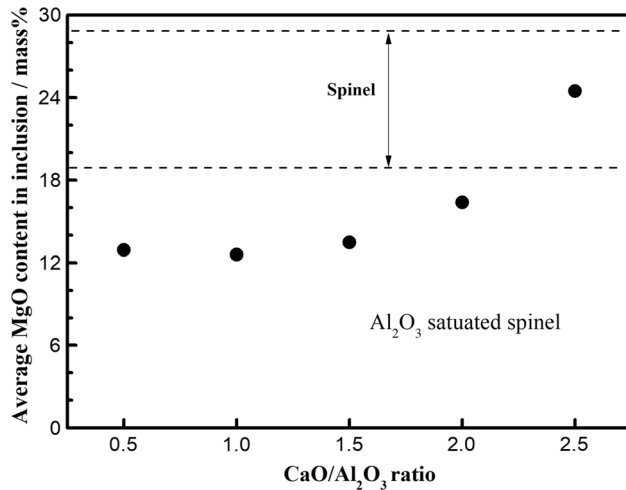


Fig. 10—Average MgO amount in inclusions observed for experiments 1 and 4–7.

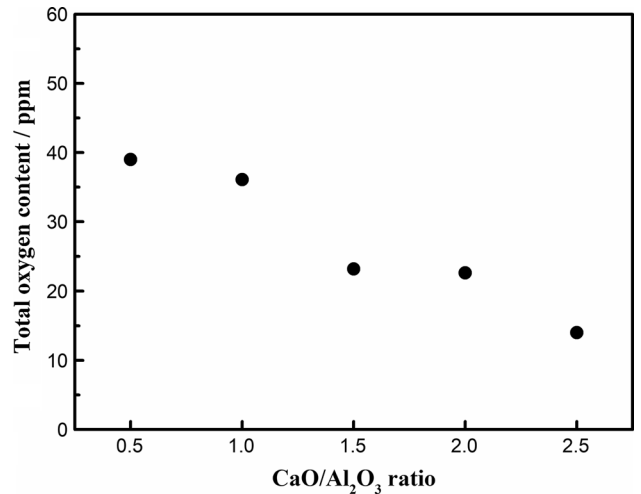


Fig. 11—Total oxygen content in steel after reaction for experiments 1 and 4–7.

Table III. Typical Published Mg-O Thermodynamic Data

| Researcher            | Ohta <i>et al.</i> <sup>[20]</sup> | Itoh <i>et al.</i> <sup>[21]</sup> | Han <i>et al.</i> <sup>[22]</sup> | Du <i>et al.</i> <sup>[23]</sup> |
|-----------------------|------------------------------------|------------------------------------|-----------------------------------|----------------------------------|
| $\lg K_{Mg}$ (1873 K) | - 7.86                             | - 6.8                              | - 6.03                            | - 8.07                           |

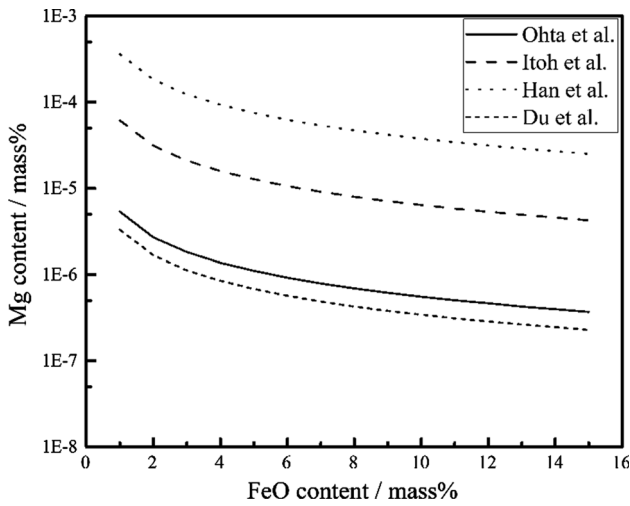


Fig. 12—Equilibrated Mg content in steel with different FeO amounts in slag.

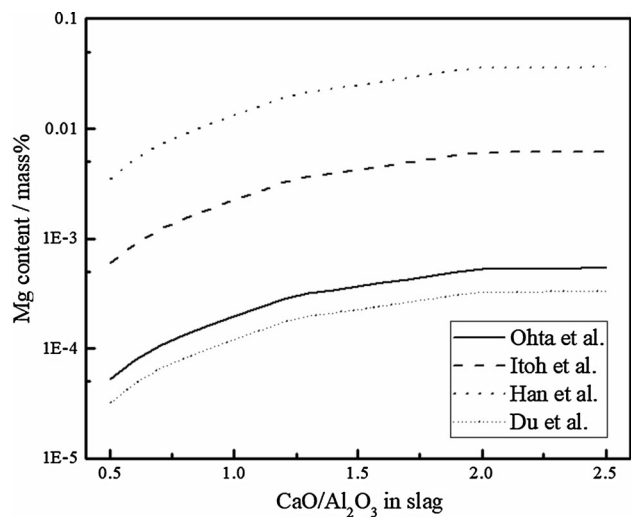


Fig. 14—Equilibrated Mg content in steel with different CaO/Al<sub>2</sub>O<sub>3</sub> ratios in slag.

Table IV. Cited Interaction Coefficients

| $e_j^i$ | $i$    |    |       |    |
|---------|--------|----|-------|----|
|         | O      | Mg | Al    | Ti |
| Mg      | - 3    | 0  | 0     | 0  |
| Al      | - 1.98 | 0  | 0.043 | 0  |

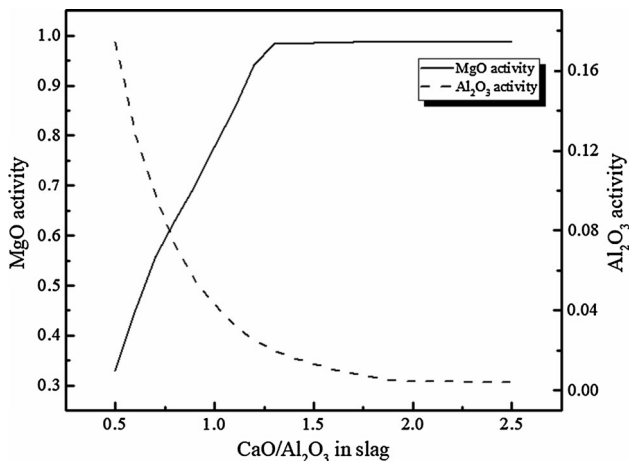


Fig. 13—Effects of CaO/Al<sub>2</sub>O<sub>3</sub> ratio on MgO and Al<sub>2</sub>O<sub>3</sub> activities in slag.

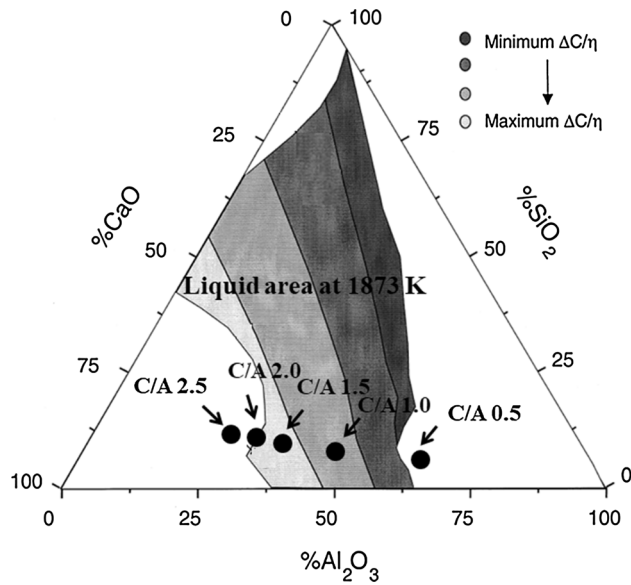


Fig. 15—Projection of the slag composition into Al<sub>2</sub>O<sub>3</sub>-CaO-SiO<sub>2</sub> system at 1873 K.

priority of occurrence of Reaction [1] explains the critical amount of FeO on the formation behavior of spinel inclusions. In this study, spinel inclusions were observed in experiment 1, and only Al<sub>2</sub>O<sub>3</sub> inclusions were observed in experiments 2 and 3, which indicate that the 4 pct FeO was not reduced to an extremely low amount during the reaction time. The supply of Mg



from the top slag could be hindered by the increasing FeO amount in the slag; however, the cleanliness of the steel (T.O) will become poor.

As shown in Figure 10, the average amount of MgO in the inclusions increased gradually with the C/A ratio in the slag, indicating that the Mg amount in the steel also increased gradually with this C/A ratio. The Mg was supplied from the top slag to the steel through Reaction [2]. According to Reaction [2], the increase in Mg is due to the increasing ratio of  $a_{\text{MgO}}^3/a_{\text{Al}_2\text{O}_3}$  as the Al amount and initial FeO amount in the slag were the same for all experiments conducted. The changes in the activities of MgO and  $\text{Al}_2\text{O}_3$  in slag with different C/A ratios are shown in Figure 13. With the increasing C/A ratio, the activity of the MgO gradually increased to unity (referred to as a pure solid substance) and then stabilized, whereas that of the  $\text{Al}_2\text{O}_3$  gradually decreased and then stabilized when the C/A was over 2.0. The calculated Mg content equilibrated with slag of a different C/A is shown in Figure 14. As Figure 14 indicates, the Mg amount increased gradually with the C/A ratio in the slag and stabilized when the C/A ratio reached over 2.0, and the calculated Mg content even varied with the different amounts of  $K_{\text{Mg}}$ . However, as shown in Figure 10, the average amount of MgO in the inclusions increased gradually and did not stabilize when the C/A was over 2.0, the reason for which remains unclear, necessitating a future study in this area.

Apart from the increase in Mg with the C/A ratio, the cleanliness of the steel improved gradually, and the observed inclusion type changed from  $\text{Al}_2\text{O}_3$  to spinel. In this study, only  $\text{Al}_2\text{O}_3$  and spinel inclusions were observed, which have almost the same physical properties. Therefore, the improvement of the cleanliness was caused by the improvement of the inclusion-absorption capability of the slag, rather than the inclusion type. M. Valdez<sup>[16]</sup> investigated the capability of  $\text{Al}_2\text{O}_3$ -CaO-SiO<sub>2</sub> slag to absorb solid oxide inclusions. According to the calculation results, a  $\text{Al}_2\text{O}_3$ -CaO-SiO<sub>2</sub> phase diagram was divided into four regions according to their inclusion-absorption capability ( $\Delta C/\eta$ , where  $\Delta C$  is the super saturation, and  $\eta$  is the slag viscosity), as shown in Figure 15.<sup>[16]</sup> The slag compositions in this study were normalized and projected in the  $\text{Al}_2\text{O}_3$ -CaO-SiO<sub>2</sub> phase diagram, as indicated in Figure 15. It is clear that the inclusion-absorption capability increased with the C/A ratio in slag, which explains the improvement of the cleanliness of the steel.

## V. CONCLUSIONS

In this study, Al-killed steel reacted with CaO- $\text{Al}_2\text{O}_3$ -SiO<sub>2</sub>-MgO-FeO slag, and the effects of the FeO content and C/A ratio on the inclusion formation behavior were clarified; the following conclusions can be drawn.

1. After the slag/steel reaction, MgO- $\text{Al}_2\text{O}_3$  spinel inclusions formed in certain cases. The Mg source for

the spinel inclusion formation was the MgO-containing slag rather than the MgO crucible.

2. The Al in the steel reacted with FeO with priority, and a Mg supply reaction occurred only when the FeO content in the slag was reduced to a low concentration. With the decrease in the initial content of FeO in the slag, the inclusions formed changed from  $\text{Al}_2\text{O}_3$  to spinel, and the cleanliness of the steel increased.
3. With the increasing C/A ratio in the slag, the average MgO amount in the observed inclusions increased, and all of the inclusions changed to spinel when the C/A ratio was 2.5 and the initial FeO amount was 2 pct. In addition, the cleanliness of the steel (T.O content) improved with the C/A ratio as the inclusion-absorption capability of the slag increased.

## ACKNOWLEDGMENTS

The authors are grateful for financial support from the National Key R&D Program of China (2017YFB0304000 & 2017YFB0304001).

## REFERENCES

1. H. Tanaka, R. Nishihara, I. Kitagawa, and R. Tsujino: *ISIJ Int.*, 1993, vol. 33, pp. 1238–43.
2. K. Reitmann, A. Kursfeld, U. Muschner, and H. Holzgruber: *2nd European Continuous Casting Conference*, Düsseldorf, 20–22 June 1994, Proceedings, vol. 1, p. 141.
3. K.K. Lee, J.M. Park, J.Y. Chung, S.H. Choi, and S.B. Ahn: *La Revue de Métallurgie-CIT*, 1996, pp. 503–509.
4. M. Kitamura, T. Soejima, S. Koyama, Y. Matsuda, J. Abu, and Y. Nimiya: *ISIJ Int.*, 1994, vol. 24, pp. 966–72.
5. Y. Qin, X. Wang, L. Li, and F. Huang: *Steel Res. Int.*, 2015, vol. 86, pp. 1037–45.
6. L. Zhang and B. Thomas: *ISIJ Int.*, 2003, vol. 43, pp. 271–91.
7. C. Liu, F. Huang, J. Suo, and X. Wang: *Metall. Mater. Trans. B*, 2016, vol. 47B, pp. 989–98.
8. C. Liu, F. Huang, and X. Wang: *Metall. Mater. Trans. B*, 2016, vol. 47B, pp. 999–1009.
9. C. Liu, X. Gao, S. Ueda, and S.Y. Kitamura: *ISIJ Int.*, 2018, vol. 58, pp. 488–95.
10. K.J. Graham and G.A. Irons: *AISTech 2009 Proceedings*, pp. 1003–11.
11. J. Mendez, A. Gomez, C. Capurro, R. Donayo, and C. Cicutti: *Clean Steel 8 Conference 2012*, Budapest.
12. C. Cicutti, C. Capurro, and G. Cerrutti: *Clean Steel 9 Conference 2015*, Budapest.
13. G. Chen, Y. Guo, and S. He: *Metall. Res. Technol.*, 2016, vol. 113 (204), pp. 1–10.
14. J.-Y. Choi and H.-G. Lee: *ISIJ Int.*, 2003, vol. 43, pp. 1348–55.
15. J.-Y. Choi, H.-G. Lee, and J.-S. Kim: *ISIJ Int.*, 2002, vol. 42, pp. 852–60.
16. M. Valdez, G.S. Shannon, and S. Sridhar: *ISIJ Int.*, 2006, vol. 46, pp. 450–57.
17. B.H. Reis, W.V. Bielefeldt, and A.C.F. Vilela: *J. Mater. Res.*, 2014, vol. 3, pp. 179–85.
18. B.J. Monaghan and L. Chen: *Ironmak. Steelmak.*, 2006, vol. 33 (4), pp. 323–30.
19. A. Harada, G. Miyano, N. Maruoka, H. Shibata, and S.-Y. Kitamura: *ISIJ Int.*, 2014, vol. 54, pp. 2230–38.

20. H. Ohta and H. Suito: *Metall. Mater. Trans. B*, 1997, vol. 28B, pp. 1131–39.
21. H. Itoh, M. Hino, and S. Ban-ya: *Tetsu-to-Hagane*, 1997, vol. 83, pp. 623–28.
22. Q. Han, D. Zhou, and C. Xiang: *Steel Res. Int.*, 1997, vol. 68, pp. 9–14.
23. J. Gran and S. Du: *Metall. Mater. Trans. B*, 2011, vol. 32B, pp. 921–24.
24. M. Hino and K. Ito: *Thermodynamic Data for Steelmaking: The 19th Committee in Steelmaking*, The Japan Society for Promotion of Science, Tokyo, 2010.